

Sakarya Üniversitesi Fen Bilimleri Dergisi
Sakarya University Journal of Science

e-ISSN : 2147-835X
Publisher : Sakarya University

Vol. 30, No. 2, 158-165, 2026
DOI: 10.16984/saufenbilder.1760764

Research Article

Synthesis of ZrB_2 by Carbothermic Method with Reactant Material Obtained from Polymer Precursor

Oğuz Karaahmet

Cerative, Yıldız Technical University Davutpasa Campus Technology Development Zone, 34220, Esenler, İstanbul, Türkiye, ogkaraahmet@gmail.com

ARTICLE INFO

Keywords
Polymeric precursor
Boron source
Reactant
Glassy B_2O_3
Carbothermal reduction

Article History
Received: 11.08.2025
Revised: 26.11.2025
Accepted: 10.03.2026
Online Available:21.04.2026

ABSTRACT

Zirconium diboride (ZrB_2) was synthesized via a carbothermic method using a ZrO_2 powder mixture, which was obtained a reactant by mixing B_2O_3 and a carbon source derived from a polymer precursor as well as by combining glassy B_2O_3 with activated carbon. The polymer precursor was calcined to obtain the reactant powder. ZrB_2 particles were synthesized with two different temperatures (1400 °C and 1500 °C). At 1500 °C, the product mainly consisted of short, cubic and prismatic grains exhibiting agglomerated morphologies, wheras at 1400 °C, longer rod-like grains and agglomerated prismatic structures were observed. The final products contained impurities such as ZrO_2 and ZrC. ZrB_2 with rod-like morphology was synthesized at different temperatures using the reactant. It was observed that the particle size decreased with increasing synthesis temperature. A higher synthesis temperature also reduced the amount of residual ZrO_2 and increased ZrC formation, likely due to boron source deficiency at high temperatures.

1. Introduction

Zirconium diboride (ZrB_2) is a transition metal diborides (MB_2) and as one of the ultra-high temperature ceramics (UHTCs). It has a hexagonal crystalline structure and exhibits strong covalent bonding between zirconium and boron atoms. ZrB_2 has moderate density (6.09–6.119 g/cm³), high hardness (20–23 GPa), and high melting point (~3246 °C). It possesses a high modulus of elasticity (~495 GPa) and mechanical strength (400-600 MPa). It also displays high chemical stability, and resistance to oxidation, ablation, corrosion, erosion, and thermal shock under extreme conditions. However, it has low toughness (3–4 $MPa.m^{1/2}$) and poor sinterability [1–10]. The sinterability of ZrB_2 is limited due to its low self-diffusion coefficient, strong covalent bonding and oxygen-related contamination, which hinder effective densification during sintering processes such as hot pressing [3, 9]. ZrB_2 is widely used in thermal protection systems, components of scramjet engines for hypersonic flight, high-temperature electrodes, and molten metal containment systems. It is also used in high-speed aircraft and re-entry vehicle structures, space shuttle components, rocket propulsion systems, solar thermal receivers, cutting tools, refractory linings, and microelectronic devices [4–10].

There are various methods for synthesizing ZrB_2 such as vapor deposition, in-situ solid/liquid processes, solid-state reactions, self-propagating high-temperature synthesis, and mechanochemical synthesis. However, these techniques often involve high temperatures or long production times, which can result in coarse particles and impure final products [3, 8]. Borothermal reduction processes offer enhanced controllability and produce powders with high purity [11].

Nevertheless, the elemental raw materials are very costly; therefore, the direct reaction method becomes impractical for industrial-scale [12]. Carbothermal methods are frequently used for large-scale production; however, they require high operation temperatures and may lead to the formation of impurity phases [8, 13, 14]. The

Cite as: O. Karaahmet, "Synthesis of ZrB_2 by carbothermic method with reactant material obtained from polymer precursor," *Sakarya University Journal of Science,* vol. 30, no. 2, pp. 158-165, 2026. https://doi.org/10.16984/saufenbilder.1760764

This is an open access paper distributed under the terms and conditions of the Creative Commons Attribution-NonCommercial 4.0 International License.

carbothermal method is controllable and offers a cost-effective preparation method. The process is relatively simple, and the raw materials are inexpensive and readily available [12]. However, solid-state reactions require high synthesis temperatures, and the final powder can exhibit poor sinterability and contain impurities [15]. Self-propagating high-temperature synthesis (SHS) is an energy-efficient technique with lower processing temperatures and a simplified operation. However, the control of process can be difficult, potentially causing incomplete reactions and impurity formation [16, 17].

The sol-gel process facilitates the production of fine particles and yields final powders with high purity. Nevertheless, it suffers from reproducibility issues, and its productivity is low for large-scale of ZrB_2 powder synthesis [10, 18–20]. In addition, the production temperature can be lowered by this method. Although chemical vapor deposition (CVD) is mostly restricted to thin-film production, it ensures high purity [17]. However, its application to ZrB_2 is limited due to the complexity and operational difficulties of the process [21]. Mechanochemical synthesis enables the production of fine powders, but it is often affected by contamination and scalability limitations [17, 22, 23].

The traditional raw materials can lead to the formation of non-unifom and coarse ZrB_2 powders, which may adversely negatively affect the properties of the final product. In contrast, a polymeric precursor produced via the sol-gel method offers more homogenous and uniformly distributed raw materials. In this study, PVBO (Polyvinyl borate) was employed as a polymeric precursor and synthesized through a dehydration–condensation reaction between H_3BO_3 and PVA via the sol–gel method. In this process, –OH groups present in the PVA chain structure is removed, leading to the formation of voids within the polymer network.

During gelation, O–B–O species released as a result of the dissolution of H_3BO_3 in water diffuse through these voids and bind to sites created by the detachment of –OH groups from the C–O bonds of the PVA backbone [24, 25]. Consequently, B–O–C ester bonds are formed, resulting in a cross-linked structure, and the PVBO is synthesized (Eq. 1) [26]. The boron-based polymeric material was subsequently calcined to remove the organic components from the structures and obtain the reactants. During the thermal decomposition of PVBO, the side groups degrade first, followed by the breakdown of the main polymer chain as the temperature increases [27]. The heat treatment promotes the formation of B_2O_3 phases which are homogeneously distributed within a carbon matrix. This structure provides shorter diffusion paths, increased interfacial contact, and a homogeneous phase distribution, thereby enhancing reaction kinetics and increase the number of nucleation sites [26, 28], ultimately reducing the temperature required for ZrB_2 synthesis.

In this study, the synthesis of ZrB_2 from a reactant derived from a polymeric precursor prepared by the sol-gel method was investigated. Furthermore, the phase composition and morphology of the synthesized products were compared with those of the final product obtained using conventional raw materials.

2. General Methods

Polyvinyl alcohol (PVA 17/88), boric acid (99.92%, EtiMaden), distilled water, ZrO_2 (20–30 nm, 99%, Nanokar Nanotechnology), B_2O_3 (98%, EtiMaden, glassy), and activated carbon (1 μm, <99%, Nanografi) were used as raw materials. The synthesis process of PVBO from polyvinyl alcohol and boric acid, as well as the calcination procedure, was carried out following the methods described in references [29-31].

First, PVA was dissolved in distilled water at 60 °C (PVA:water = 2 g:60 mL) for 60 min. Separately, H_3BO_3 was dissolved in distilled water at 80 °C (H_3BO_3:water= 2 g:45 mL) for 60 min. In both cases, continuous stirring was applied using a magnetic stirrer. Gelation was then carried out at 60 °C by dropwise addition of the boric acid–water solution into the PVA–water solution under continous stirring, as given in Eq. (1). The activation energy required for gelation was provided by heating and continuous stirring. The obtained gel was dried at 120 °C for 4 h to produce PVBO in solid form [31].

$$B–(O–H)_3 + 3C_xH_yO_z–OH \rightarrow C_{3x-3}H_{3y}O_{3z}B–(O–C)_3 + 3H_2O \quad (1)$$

The PVBO material was crushed, ground into powder, and calcined at 600 °C for 60 min in a chamber-type furnace using a porcelain crucible, obtaining a black-colored reactant material as described in Eq. (2) [31].

$$2C_{3x-3}H_{3y}O_{3z}B\text{–}(O\text{–}C)_3 + (1/2)(pn+3y-6z-3)O_2 \rightarrow B_2O_3 + (6x-pm)C + pC_mO_n + 3yH_2O \quad (2)$$

The reactant was ground at 200 RPM for 10 min. When the reactant was mixed with pure water, the B_2O_3 in the structure dissolved, and remain only carbon in reactant. The carbon was filtered, dried, and its amount was measured. By subtracting the amount of carbon obtained after the B_2O_3 dissolution process from the initial sample mass, the amount of B_2O_3 was determined. The molar masses of carbon and B_2O_3 were calculated, and the C/B_2O_3 molar ratio was found to be 4.34.

$$ZrO_2 + B_2O_3 + 5C \rightarrow ZrB_2 + 5CO_{(g)} \quad (3)$$

According to Eq. (3), a homogeneous and uniform powder mixture of ZrO_2 and the reactant powder, as well as a mixture of ZrO_2, glassy B_2O_3, and activated carbon were prepared using a ball mill. The raw materials were homogenized by mixing them for 30 min at 150 RPM in an agate pot using a Retsch Planetary Ball Mill (PM100), with a maintained ball-to-powder weight ratio of 20:1. Following this process, the powder mixtures were pressed into bulk form using a uniaxial hydraulic press to produce pellets. These pellets were then placed in a graphite crucible with a lid. The synthesis process was carried out at 1400 °C and 1500 °C for 3 h in an atmosphere-controlled furnace with a heating rate of 15 °C/min under argon gas. Argon gas was continuously charged at a flow rate of 3 L/min. Both the heating and cooling phases were controlled at rates of 15 °C/min and 3 °C/min, respectively. X-ray Diffraction (XRD) analysis was performed to identify the phases of reactant, glassy B_2O_3 and synthesized powders. A XRD diffractometer (Bruker D8 Advance) equipped with CuKα radiation and a step size of 0.02° (2θ) was used for the analysis. The microstructure of the synthesized powders was investigated using Scanning Electron Microscopy (SEM) (ZEISS EVO 10) operated at an acceleration voltage of 20 kV, with a working distance ranging from 7.47 to 9.05 mm at 1000x ve 2500x magnification, and elemental analysis was conducted using Energy Dispersive Spectroscopy (EDS).

3. Results and Discussion

The XRD diffractograms of the reactant and glassy B_2O_3 were given in Figure 1. The reactant was obtained by calcining the synthesized polymeric precursor, which contains both B_2O_3 and carbon. The diffactograms show both amorphous structure and crystalline peaks. The amorphous structure results from the loss of organic components from polymeric materials during calcination. The observed crystalline peaks are associated with the B_2O_3 source. The $B(OH)_3$ was identified in the XRD pattern, as B_2O_3 easily converts to $B(OH)_3$ upon exposure to atmospheric moisture. Additionally, the structure contains a significiant amount of amorphous carbon, making it difficult to accurately determine the boron source in the sample. The phase structure of glassy B_2O_3 includes both amorphous and crystalline phases. The presence of crystalline phases is probably due to partial hydration of B_2O_3 through contact with the moisture during production or the other processing steps.

The XRD patterns of the final products synthesized at 1400 °C and 1500 °C using ZrO_2, glassy B_2O_3, and activated carbon are presented in Figure 2. At 1400 °C, the diffraction peaks indicate the presence of ZrB_2, ZrO_2, and ZrC phases. Unreacted carbon and B_2O_3 were not detected by XRD, as these materials were mostly consumed during the reaction.

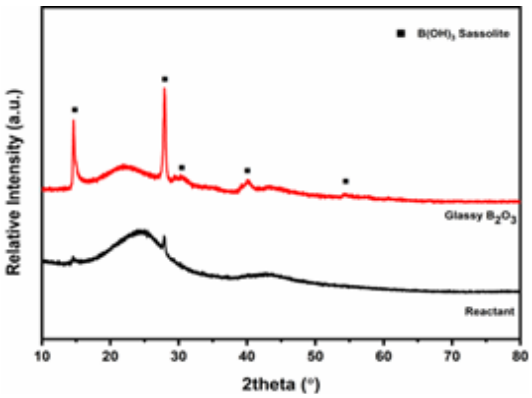

Figure 1. XRD diffractograms of the reactant and glassy B_2O_3

However, the presence of ZrO_2 indicates the Eq. (3) was not fully completed, potentially due to insufficient boron source or kinetic limitations. The appearance of ZrC in the final product is likely caused by the reaction of carbon with ZrO_2, forming the carbide phase in localized regions [4].

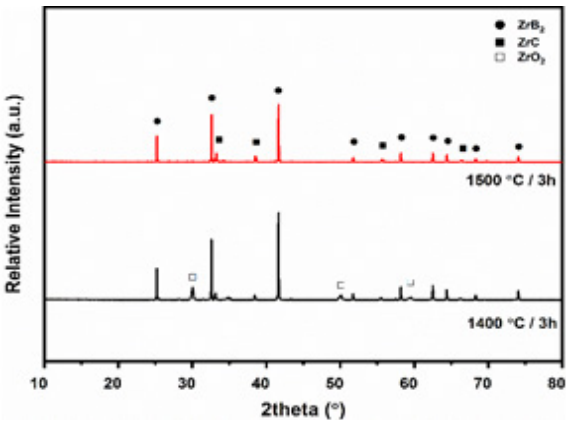

Figure 2. XRD diffractograms of samples heat-treatment at 1400 °C and 1500 °C for 3 h, prepared using glassy B_2O_3, activated carbon, and ZrO_2

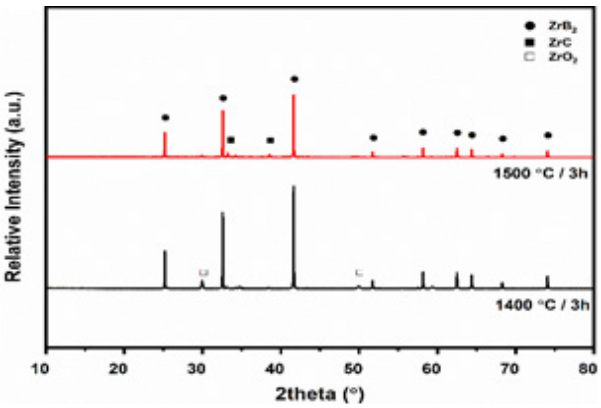

Figure 3. XRD diffractograms of a mixture prepared from the reactant and ZrO_2, heat-treated at 1400 °C and 1500 °C for 3 h

Above ~1100 °C, B_2O_3 tends to form volatile suboxides in the gas phase, leading to the loss of boron source, particularly in open or low-pressure systems. This results the reaction to not be fully completed. Furthermore, the slower reaction kinetics at 1400 °C may have limited the overall conversion, leading unreacted ZrO_2 in the final product. At 1500 °C, the synthesized product contained only a small amount of residual ZrO_2 and ZrC, while ZrB_2 phase was dominant. According to the literatures [4, 5], the formation of ZrC is associated with B_2O_3 loss from the reaction environment. However, if excess B_2O_3 are present in the reaction area, ZrC can further react with B_2O_3 and carbon to form ZrB_2 (Eq. 6). The increased intensity of ZrC peaks at 1500 °C indicates that ZrC starts to form at lower temperatures (Eq. 5), and when B_2O_3 is insufficient, it remains in the structure, limiting ZrB_2 formation. Although ZrB_2 is thermodynamically more stable than ZrC at high temperatures, ZrC may form earlier under boron-deficient conditions.

The presence of ZrB_2, ZrC, and ZrO_2 phases were identified (Figure 3) as a result of the synthesis carried out at 1400 °C using a mixture prepared from a reactant and ZrO_2. In the structure of the final product obtained from reactant, it was observed that the amount of ZrC phase was lower compared to the product synthesized directly from raw materials. At 1500 °C, a decrease in the peak intensity of ZrO_2 and an increase in the peak intensity of ZrC phase were observed, indicating a shift toward further carbide formation with increasing temperature.

$$3ZrO_2 + 6B + 6C \rightarrow 3ZrB_2 + 6CO_{(g)} \quad (4)$$

$$ZrO_2 + 3C \rightarrow ZrC + 2CO_{(g)} \quad (5)$$

$$ZrC + B_2O_3 + 2C \rightarrow ZrB_2 + 3CO_{(g)} \quad (6)$$

$$7ZrO_2 + 5B_4C \rightarrow 7ZrB_2 + 3B_2O_3 + 5CO_{(g)} \quad (7)$$

$$2ZrO_2 + B_4C + 3C \rightarrow 2ZrB_2 + 4CO_{(g)} \quad (8)$$

$$2ZrO_2 + B_2O_3 + 8C \rightarrow ZrB_2 + ZrC + 7CO_{(g)} \quad (9)$$

In this study, the reactant and glassy B_2O_3 were used as boron sources. The Gibbs free energy values of the reactions (Eqs. 3–9) were calculated using HSC 6.0 and are presented in Figure 4 and the $\Delta G°$ values for Eqs. 3-9 at 1400 °C and 1500 °C are given in Table 1. Among the evaluated boron sources, B_4C facilitates the onset of reactions at lower temperatures compared to other boron-containing raw materials. Likewise, the presence of elemental boron in the mixture promotes reactions initiation at lower temperatures than B_2O_3.

The use of a consistent carbon source, activated carbon provides a basis for a direct comparison of the reduction products formed at different temperatures depending on the boron source. Thermodynamically, the Eq. (3) is not favorable at 1400 °C ($\Delta G° > 0$ at 1400 °C). However, the physical and chemical properties of the raw materials, and the homogenization processes can increase the contact between components and faciliate the reduction process. If elemental boron and activated carbon are used as raw

materials, particularly in fine-powder form, they may initiate the reaction at lower temperatures due to kinetic effects and increased surface area between components. In this study, ZrB_2 was synthesized as a result of the reduction processes. However, secondary phases such as ZrC and unreacted ZrO_2 were also observed in the final products. The presence of unreacted ZrO_2 at 1400 °C suggests that the reduction was incomplete, likely due to reaction conditions and the relatively low temperature.

As the temperature increased to 1500 °C, the amount of residual ZrO_2 decreased, while the formation of the ZrC phase became more pronounced. This behavior can be attributed to the enhanced thermodynamic tendency of ZrC formation at higher temperature as well as the volatilization of B_2O_3 into suboxides (e.g., B_2O_2, BO) in the gas phase. If boron source is unremained in the structure, the carbon is not reduce the B_2O_3 to boron and carbon react with ZrO_2 and form ZrC. Therefore promoting the formation of ZrC phase increase depending on boron loss. When the boron source is depleted in the reaction area, carbon cannot reduce B_2O_3 to elemental boron; instead, it reacts with ZrO_2 to form ZrC. Therefore, boron loss promotes the formation of the ZrC phase.

As shown in Figure 5 (a), at 1400 °C, spherical and irregularly shaped grains were observed on the agglomerated structures. These grains were not clearly distinguishable. The final products exhibited a crystalline structure, with the presence of ZrB_2, ZrC, and ZrO_2 phases. However, scanning electron microscopy (SEM) images revealed that the grains were poorly defined and agglomerated. The persistence of the ZrO_2 phase indicates that the reduction reaction was incomplete. This agglomeration may be attributed to the presence of a residual glassy B_2O_3 phase. Glassy B_2O_3 melts between 400–700 °C and remains in the molten state at 1400 °C, allowing the reduction reaction to occur at the liquid–solid interface. During the reduction process, the raw materials–ZrO_2 and activated carbon–remain in contact with this molten phase, facilitating the reaction at the liquid–solid interface. The molten B_2O_3 may also act as a temporary binder between grains during cooling, further contributing to agglomeration.

Conversely, if B_2O_3 is fully consumed during the reduction process, the final particles would likely be less agglomerated and more loosely packed.

Nevertheless, grain sintering driven by high temperatures can also lead to agglomeration [3]. At a reduction temperature of 1500 °C, the large agglomerated structures observed at 1400 °C disappeared, and instead, multi-faceted agglomerates were formed. These grains were typically smaller than 10 µm and exhibited a non-uniform spatial distribution (Figure 5b).

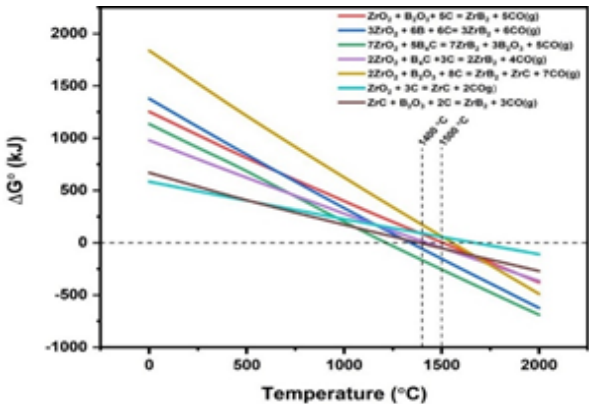

Figure 4. Enthalpy and Gibbs free energy values of the reactions (Eqs. 3-9)

In the study where a reactant material was used as the boron source, it was observed that at 1400 °C, the samples exhibited a longer rod-like grain morphology and formed agglomerated prismatic structure (Figure 6a). It can be stated that the crystals grew rapidly in a specific direction, indicating anisotropic growth [6, 10]. The grain size was approximately 10 µm and showed a heterogeneous distribution. When the temperature increased to 1500 °C, short, cubic and prismatic grains with agglomerated morphologies formed (Figure 6b). A more multidirectional growth pattern was observed. The grain size was below 10 µm and exhibit a nearly homogeneous distribution.

4. Conclusion

A polymer-derived reactant and a mixture of glassy B_2O_3 with activated carbon can be effectively used as boron and carbon sources in the synthesis of ZrB_2. The final products exhibited similar phase and morphological characteristics. Therefore, the polymer-derived reactant represents a viable alternative to conventional raw materials. The final product contained unreacted ZrO_2 at 1400 °C, a behavior primarily associated with insufficient boron availability under the given synthesis conditions. However, increasing the synthesis temperature to 1500 °C enabled the complete reduction of ZrO_2,

with ZrC remaining as a minor secondary phase. ZrB_2 grains synthesized at 1400 °C were coarser (~10 μm) and exhibited precursor-dependent morphological variations, whereas those formed at 1500 °C were finer and predominantly cubic.

Table 1. ΔG° values of Eqs. 3-9 at 1400 °C and 1500 °C

ΔG° (kj)	**1400 °C**	**1500 °C**
$ZrO_2 + B_2O_3 + 5C \rightarrow ZrB_2 + 5CO_{(g)}$	81.992	4.271
$3ZrO_2 + 6B + 6C \rightarrow 3ZrB_2 + 6CO_{(g)}$	-58.668	-153.944
$7ZrO_2 + 5B_4C \rightarrow 7ZrB_2 + 3B_2O_3 + 5CO_{(g)}$	-166.484	-255.255
$2ZrO_2 + B_4C + 3C \rightarrow 2ZrB_2 + 4CO_{(g)}$	15.898	-48.488
$2ZrO_2 + B_2O_3 + 8C \rightarrow ZrB_2 + ZrC + 7CO_{(g)}$	171.727	60.5
$ZrO_2 + 3C \rightarrow ZrC + 2CO_{(g)}$	89.735	56.229
$ZrC + B_2O_3 + 2C \rightarrow ZrB_2 + 3CO_{(g)}$	89.735	56.229

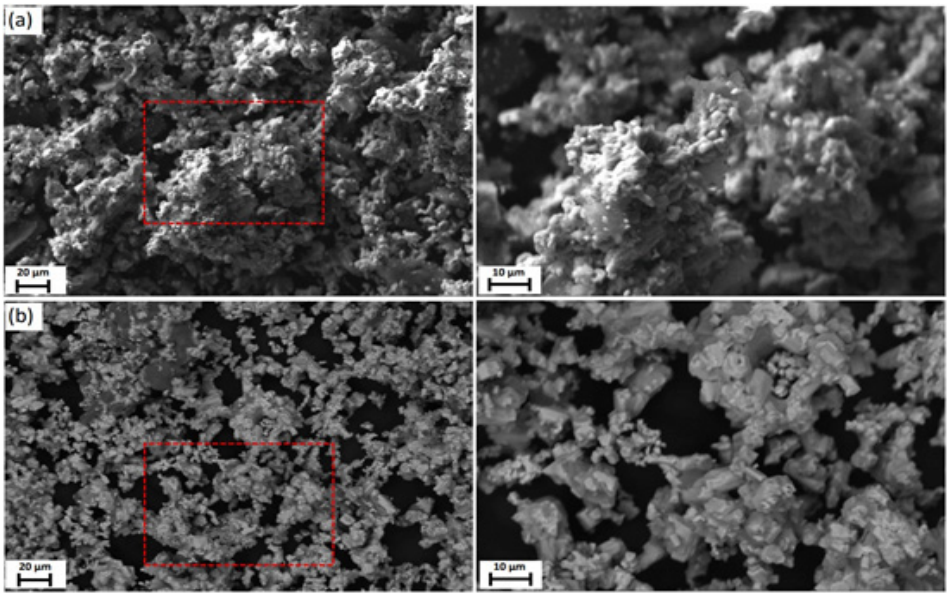

Figure 5. FESEM images of the glassy B_2O_3, activated carbon, and ZrO_2 after heat treatment at (a) 1400 °C for 3 h (b) 1500 °C for 3 h (The region marked with a red square is shown at higher magnification in the image on the right)

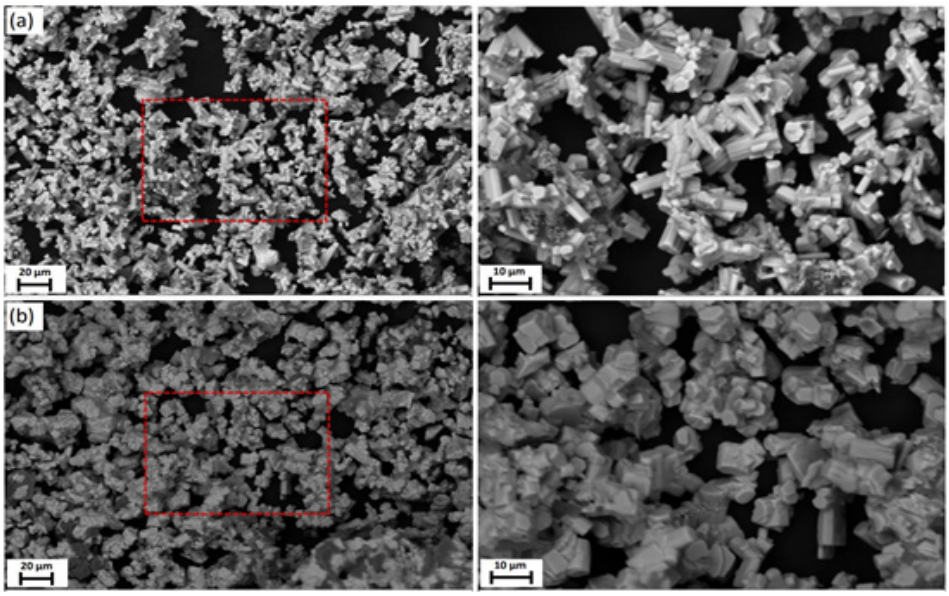

Figure 6. FESEM images of the reactant and ZrO_2 after heat treatment at (a) 1400 °C for 3 h (b) 1500 °C for 3 h. (The region marked with a red square is shown at higher magnification in the image on the right)

Article Information Form

The Declaration of Conflict of Interest/ Common Interest

No conflict of interest or common interest has been declared by authors.

Artificial Intelligence Statement

During the preparation of this work, the author used ChatGPT solely for the purpose of English language editing. No artificial intelligence tools were employed in the generation, analysis, or interpretation of the scientific content.

Copyright Statement

Authors own the copyright of their work published in the journal and their work is published under the CC BY-NC 4.0 license.

References

[1] A. C. Murchie, J. L. Watts, W. G. Fahrenholtz, and G. E. Hilmas, "Mechanical properties of borothermally synthesized zirconium diboride at elevated temperatures," *Int. J. Appl. Ceram. Technol*., vol. 18, no. 4, pp. 1235–1243, Mar. 2021, doi: 10.1111/ijac.13755.

[2] W. M. Guo and G. J. Zhang, "New borothermal reduction route to synthesize submicrometric ZrB_2 powders with low oxygen content," *J. Am. Ceram. Soc*., vol. 94, no. 1, pp. 3702–3705, Oct. 2011, doi: 10.1111/j.1551-2916.2011.04869.x.

[3] S. Ran, O. Van der Biest, and J. Vleugels, "ZrB_2 powders synthesis by borothermal reduction," *J. Am. Ceram. Soc*., vol. 93, no. 6, pp. 1586–1590, Jun. 2010, doi: 10.1111/j.1551-2916.2010.03747.x.

[4] W. M. Guo and G. J. Zhang, "Reaction processes and characterization of ZrB_2 powder prepared by boro/carbothermal reduction of ZrO_2 in vacuum," *J. Am. Ceram. Soc*., vol. 92, no. 1, pp. 264–267, Jan. 2009, doi: 10.1111/j.1551-2916.2008.02836.x.

[5] C. Hu, J. Zou, Q. Huang, G. Zhang, S. Guo, and Y. Sakka, "Synthesis of plate-like ZrB_2 grains," *J. Am. Ceram. Soc*., vol. 95, no. 1, pp. 85–88, Dec. 2012, doi: 10.1111/j.1551-2916.2011.04990.x.

[6] H. T. Liu, H. Y. Qiu, W. M. Guo, J. Zou, and G. J. Zhang, "Synthesis of rod-like ZrB_2 powders," *Adv. Appl. Ceram*., vol. 114, no. 8, pp. 418–422, Dec. 2015, doi: 10.1179/1743676114Y.0000000223.

[7] C. Xie, M. Chen, X. Wei, M. Ge, and W. Zhang, "Synthesis and microstructure of zirconium diboride formed from polymeric precursor pyrolysis," *J. Am. Ceram. Soc*., vol. 95, no. 3, pp. 866–869, Jan. 2012, doi: 10.1111/j.1551-2916.2011.05060.x.

[8] E. Y. Jung, J. H. Kim, S. H. Jung, and S. C. Choi, "Synthesis of ZrB_2 powders by carbothermal and borothermal reduction," *J. Alloys Compd*., vol. 538, pp. 164–168, May 2012, doi: 10.1016/j.jallcom.2012.05.076.

[9] G. S. An, J. S. Han, J. U. Hur, and S. C. Choi, "Synthesis of sub-micro sized high purity zirconium diboride powder through carbothermal and borothermal reduction method," *Ceram. Int.*, vol. 43, no. 8, pp. 5896–5900, Jan. 2017, doi: 10.1016/j.ceramint.2017.01.068.

[10] Z. Chen *et al.,* "Synthesis of rod-like ZrB_2 crystals by boro/carbothermal reduction," *Ceram. Int*., vol. 45, no. 11, pp. 13726–13731, May 2019, doi: 10.1016/j.ceramint.2019.04.068.

[11] M. Emamalizadeh, M. Mahdavi, and A. Shokrolahi, "Synthesis and characterization of ZrB_2 nanopowders via metallothermic reduction of ZrC_{14} using Na, Mg and Al in mild temperature: a morphology/reductant correlation," *J. Mater. Res. Technol*., vol. 9, no. 4, pp. 7686–7700, Jun. 2020, doi: 10.1016/j.jmrt.2020.04.100.

[12] L. Bai and Y. Ouyang, F. Yuan, "Progress in preparation of ZrB_2 nanopowders based on traditional solid-state synthesis," *Nanomaterials*, vol. 11, no. 9, p. 2345, Sep. 2021, doi: 10.3390/nano11092345.

[13] S. Song, R. Li, L. Gao, C. Sun, P. Hu, and Q. Zhen, "Synthesis and growth behavior of micron-sized rod-like ZrB_2 powders," *Ceram. Int*., vol. 44, no. 5, pp. 4640–4645, Feb. 2018, doi: 10.1016/j.ceramint.2017.12.026.

[14] J. Liu, Z. Huang, C. Huo, F. Li, H. Zhang, and S. Zhang, "Low-temperature rapid synthesis of rod-like ZrB_2 powders by molten-salt and microwave co-assisted carbothermal reduction," *J. Am. Ceram. Soc*., vol. 99, no. 9, pp. 2895–2898, Aug. 2016, doi: 10.1111/jace.14414.

[15] X. Yang, W. Han, T. Zhao, and R. Li, "The effects of partially or fully linked boron with a cross-linking structure of an organic precursor on the purity and morphology of ZrB_2 powder," *RSC Adv*., vol. 14, no. 2, pp. 889–901, Jan. 2024, doi: 10.1039/D3RA06932J.

[16] A. K. Khanra, L. C. Pathak, and M. M. Godkhindi, "Double SHS of ZrB_2 powder," *J. Mater. Process.*

Technol., vol. 202, no. 1-3, pp. 386–390, Oct. 2008, doi: 10.1016/j.jmatprotec.2007.09.007.

[17] J. K. Sonber and A. K. Suri, "Synthesis and consolidation of zirconium diboride: Review," *Adv. Appl. Ceram*., vol. 110, no. 6, pp. 321–334, Nov. 2011, doi: 10.1179/1743676111Y.0000000008.

[18] L. Yuan, C. Wang, M. Bi, S. Ma, and X. Weng, "Effect of processing parameters on the formation process of nano-sized ZrB_2 powders by the high energy ball milling," *Adv. Appl. Ceram*., vol. 118, no. 7, pp. 395–402, May 2019, doi: 10.1080/17436753.2019.1616979.

[19] Y. Yan, Z. Huang, S. Dong, and D. Jiang, "New route to synthesize ultra-fine zirconium diboride powders using inorganic–organic hybrid precursors," *J. Am. Ceram. Soc*., vol. 89, no. 11, pp. 3585–3588, Sep. 2006, doi: 10.1111/j.1551-2916.2006.01269.x.

[20] Y. Zhang *et al.,* "Morpholo gy evolution of ZrB_2 nanoparticles synthesized by sol–gel method," *J. Solid State Chem*., vol. 184, no. 8, pp. 2047–2052, May 2011, doi: 10.1016/j.jssc.2011.05.040.

[21] Y. Zhu, L. Cheng, M. Li, B. Ma, Y. Liu, and L. Zhang, "The synthesis and characterization of CVD ZrB_2 coating from ZrC_{l4}-BC_{l3}-H_2-Ar system," *Ceram. Int*., vol. 44, no. 2, pp. 2002–2010, Nov. 2018, doi: 10.1016/j.ceramint.2017.10.145.

[22] S. Zhang, M. Khangkhamano, H. Zhang, and H. A. Yeprem, "Novel synthesis of ZrB_2 powder via molten-salt-mediated magnesiothermic reduction," *J. Am. Ceram. Soc*., vol. 97, no. 6, pp. 1686–1688, Apr. 2014, doi: 10.1111/jace.12945.

[23] T. Simsek, M. Baris, A. K. Chattopadhyay, O. Sadan, and A. Akkurt, "Characterization of mechanochemically synthesized ZrB_2 nanocrystals with Zr/ZrO_2, B_2O_3, and Mg reactants," *Inorg. Nano-Metal Chem*., vol. 52, no. 2, pp. 262–269, Mar. 2022, doi: 10.1080/24701556.2021.1893332.

[24] S. Mondal and A. K. Banthia, "Low-temperature synthetic route for boron carbide," *J. Eur. Ceram. Soc.*, vol. 25, no. 2-3, pp. 287–291, Sept. 2005, doi: 10.1016/j.jeurceramsoc.2004.08.011.

[25] A. Fathi, N. Ehsani, M. Rashidzadeh, H. Baharvandi, and A. Rahimnejad, "Synthesis of boron carbide nano particles using polyvinyl alco hol and boric acid," *Ceram.-Silik*., vol. 56, no. 1, pp. 32–35, Dec. 2012.

[26] M. Kakiage, N. Tahara, I. Yanase, and H. Kobayashi, "Low-temperature synthesis of boron carbide powder from condensed boric acid–glycerin product," *Mater. Lett*., vol. 65, no. 12, pp. 1839–1841, Mar. 2011, doi: 10.1016/j.matlet.2011.03.046.

[27] P. M. Barros, I. V. P. Yoshida, and M. A. Schiavon, "Boron-containing poly(vinyl alcohol) as a ceramic precursor," *J. Non-Cryst. Solids*, vol. 352, pp. 3444–3450, Aug. 2006, doi: 10.1016/j.jnoncrysol.2006.02.108.

[28] M. Kakiage, N. Tahara, Y. Tominaga, S. Yanagidani, I. Yanase, and H. Kobayashi, "Effect of molecular structure of polyols with different molecular characteristics on synthesis of boron carbide powder" *Key Eng. Mater*., vol. 534, pp. 61–65, Jan. 2013, doi: 10.4028/www.scientific.net/KEM.534.61.

[29] O. Karaahmet and B. Çiçek, "Use of partially hydrolyzed PVA for boron carbide synthesis from polymeric precursor," *Ceram.-Silik*., vol. 64, no. 4, pp. 434–446, Jun. 2020, doi: 10.13168/cs.2020.0031.

[30] O. Karaahmet and B. Çiçek, "Effect of mechanically modification process on boron carbide synthesis from polymeric precursor method," *Ceram. Int*., vol. 48, no. 9, pp. 11940–11952, Mar. 2022, doi: 10.1016/j.ceramint.2022.01.043.

[31] X. W. Chen, S. M. Dong, Y. M. Kan, H. J. Zhou, J. B. Hu, and Y. S. Ding, "Effect of glycerine addition on the synthesis of boron carbide from condensed boric acid–polyvinyl alcohol precursor," *RSC Adv*., vol. 6, no. 11, pp. 9338–9343, Jan. 2016, doi: 10.1039/C5RA23303H.